# Separation of Recollision Mechanisms in Nonsequential Strong Field Double Ionization of Ar: The Role of Excitation Tunneling

B. Feuerstein,[1] R. Moshammer,[1,2] D. Fischer,[1] A. Dorn,[2] C. D. Schröter,[2] J. Deipenwisch,[1]
J. R. Crespo Lopez-Urrutia,[1] C. Höhr,[1] P. Neumayer,[3] J. Ullrich,[1,2]
H. Rottke,[4] C. Trump,[4] M. Wittmann,[4] G. Korn,[4] and W. Sandner[4]

[1]*Universität Freiburg, Hermann-Herder-Strasse 3, D-79104 Freiburg, Germany*
[2]*Max-Planck-Institut für Kernphysik, Saupfercheckweg 1, D-69117 Heidelberg, Germany*
[3]*Gesellschaft für Schwerionenforschung (GSI), D-64291 Darmstadt, Germany*
[4]*Max-Born-Institut, Max-Born-Strasse 2a, D-12489 Berlin, Germany*

(Received 5 April 2001; published 9 July 2001)

Vector momentum distributions of two electrons created in double ionization of Ar by 25 fs, 0.25 PW/cm$^2$ laser pulses at 795 nm have been measured using a "reaction microscope." At this intensity, where nonsequential ionization dominates, distinct correlation patterns are observed in the two-electron momentum distributions. A kinematical analysis of these spectra within the classical "recollision model" revealed an $(e, 2e)$-like process and excitation with subsequent tunneling of the second electron as two different ionization mechanisms. This allows a qualitative separation of the two mechanisms demonstrating that excitation-tunneling is the dominant contribution to the total double ionization yield.

DOI: 10.1103/PhysRevLett.87.043003 PACS numbers: 32.80.Rm, 31.90.+s, 32.80.Fb

Since the first observation of surprisingly high ion yields in double and multiple ionization in strong, linearly polarized laser pulses more than 15 years ago [1] many-electron dynamics in intense laser fields has been the subject of a large number of theoretical and experimental investigations (for a review, see [2]). Considering that theoretical predictions based on the "single active electron" model, assuming sequential ionization of independent electrons, fail by many orders of magnitude, it was agreed that a "nonsequential" (NS) ionization mechanism has to incorporate the correlated dynamics of two (or more) electrons in the strong laser field.

Experimental imaging techniques [3], combined with recent progress in laser development, succeeded in measuring momentum distributions of multiply charged ions for He [4], Ne [5], and Ar [6]. It was shown that mechanisms based on an instantaneous release of two (or more) electrons at a phase where the field maximizes, such as "shakeoff" [7] or "collective tunneling" [8], can be ruled out as a dominant contribution to NS double ionization. Whereas these processes lead to an ion momentum distribution along the laser polarization axis peaking at zero, the observed spectra exhibit distinct maxima at nonzero momenta [4,5]. The positions of these maxima are in accord with kinematical constraints set by the classical "rescattering model" [5,9] which was originally proposed by Corkum [10] eight years ago. In this model the first ionized electron is driven back by the oscillating laser field to its parent ion causing the ionization of a second electron in an $(e, 2e)$-like process. The experimental results settled the controversial debate on the mechanisms responsible for NS multiple ionization and stimulated a series of theoretical papers [11–14], which all include the $(e, 2e)$ recollision mechanism and, thus, support the widely accepted evidence that rescattering dominates multiple ionization in the intensity regimes investigated.

Since ion momentum distributions alone do not give complete information on the $(e, 2e)$ process during recollision, the interest focused on the correlation of the electrons emitted by an atom in the strong laser field. Very recently, coincident momentum distributions of two electrons have been determined for double ionization of Ar [15]. The investigation of strong-field double ionization of argon is of special interest because a systematic experimental study of the intensity dependence of the ion momentum distributions along the laser polarization axis for an intensity range from 0.2 to 2 PW/cm$^2$ [6] revealed distinct differences in the shape of these distributions compared to theoretical predictions either based on simple classical considerations [9] or on recent quasiclassical calculations [11,13]. Instead of a double-peak structure which should become more pronounced with decreasing laser intensity the observed distributions show only one broad peak around zero momentum. A similar behavior was found for He [4].

The observation that the minimum between the two peaks is filled with decreasing laser intensity is closely related to the question of a threshold intensity where the maximum kinetic energy of the rescattered electron becomes equal to the ionization potential of the singly charged ion. Experimentally, no such threshold effect has ever been observed. In contrast to a classical approach the quantum-mechanical description avoids the problem of a threshold intensity: the absorption of a corresponding number of photons by the first ionized electron provides the energy needed for double ionization. Indeed, a "sawtooth structure" appears in the calculated ion momentum distributions at intensities below the classical threshold (Fig. 2 of [13]) which reflects the discrete energy transfer

  

from the laser field to the atom and demonstrates nicely the transition from the classical-field regime to the multiphoton domain. It has been pointed out repeatedly [9,13,15] that electron impact excitation during the recollision with subsequent electric field (tunnel) ionization of the excited electron may also contribute significantly to double ionization. This has been already demonstrated for He in a recent semiquantitative calculation [16]. Because of its sequential nature the excitation-tunneling mechanism tends to fill up the minimum in the momentum distribution.

In order to clarify this question we present a detailed kinematical analysis on the correlated electron momenta for argon double ionization at an intensity of 0.25 PW/cm$^2$. It will be demonstrated that a kinematically complete experiment allows one to identify and separate contributions from two types of recollision mechanisms—$(e,2e)$ and excitation tunneling.

The experiments were performed at the Max-Born-Institut in Berlin using pulses of a Kerr-lens mode locked Ti:sapphire laser at 795 nm wavelength amplified to pulse energies up to 500 $\mu$J at 1 kHz repetition rate. The width of the amplified pulses was 25 fs.

Focused by a spherical on-axis mirror ($f = 100$ mm) to a spot size of 10 $\mu$m diameter (FWHM) in an ultrahigh vacuum chamber ($7 \times 10^{-11}$ mbar), it was possible to achieve pulse peak intensities of up to 25 PW/cm$^2$. Intensity fluctuations were controlled throughout the experiment and kept below 5%. The laser beam was focused on a low-density ($10^8$ atoms/cm$^3$) supersonic Ar jet which was collimated to a rectangular shape of $0.2 \times 4$ mm$^2$ at the focal spot. The wide side of the jet was oriented perpendicular with respect to the laser beam thus yielding an overlap volume between laser beam and Ar jet of 200 $\mu$m length and 10 $\mu$m diameter.

Vector momenta of ions and electrons emerging from the source volume were recorded using a "reaction microscope" which has been described in detail before [17]. All electrons with transverse energies below 30 eV and longitudinal energies below 15 eV were detected with $4\pi$ solid angle of acceptance. The ion momentum resolution along the jet expansion axis was limited by the internal jet temperature to 0.3 a.u. Transverse to the jet axis a resolution of 0.1 a.u. was achieved due to collimation of the atomic beam. In order to ensure that electrons and ions detected in each laser shot emerged from the same atom, the target and rest gas densities had to be low enough to have less than one ionization event per laser pulse occurring.

The final momentum $\vec{p}_{\mathrm{final}}$ of an electron emitted from an atom in a strong, linearly polarized laser pulse is the sum of the drift momentum $\vec{p}_{\mathrm{drift}}$ due to the acceleration in the field and the initial momentum $\vec{p}_{\mathrm{initial}}(t_1)$ of the electron starting at time $t_1$. The drift momentum depends on the phase $\phi = \omega t_1$ where the electron was born in the oscillating electric field $\vec{E}(t) = \vec{E}_0(t)\sin(\omega t)$ through $\vec{p}_{\mathrm{drift}} = \omega^{-1}\vec{E}_0(t_1)\cos(\omega t_1)$. After an $(e,2e)$ process during recollision both electrons receive the same drift momentum. The initial momenta $\vec{p}^{\,(1)}_{\mathrm{initial}}$, $\vec{p}^{\,(2)}_{\mathrm{initial}}$ of the two electrons depend on the dynamical parameters of the $(e,2e)$ process itself, i.e., on the excess energy of the recolliding electron, energy sharing, and the emission angles. Thus, the $(e,2e)$ final two-particle momentum state just after the recollision is simply shifted by $\vec{p}_{\mathrm{drift}}$ for each of the electrons yielding the finally observed correlated two electron momentum patterns. Since only the momentum components $p_1^{\parallel}$, $p_2^{\parallel}$ parallel to the polarization direction are affected by acceleration in the laser field, the perpendicular components $p_1^{\perp}$, $p_2^{\perp}$ remain unchanged directly reflecting the $(e,2e)$ dynamics. This also holds true for the momentum difference $\vec{p}_- = \vec{p}_1 - \vec{p}_2$ since the identical drift momenta cancel each other [15].

We now consider the correlated electron momentum spectra for the parallel component. Because of energy conservation we get for a given phase $\omega t_1$ as kinematically allowed regions two circles with radius $\sqrt{2E_{\mathrm{exc}}}$ centered on the diagonal with equal drift momenta $\vec{p}_{\mathrm{drift}}(t_1)$ as illustrated in Fig. 1(a). Here, $E_{\mathrm{exc}}$ is the excess energy of the $(e,2e)$ process. Superposition of the circles for all phases where the energy of the recolliding electron exceeds the ionization potential of the singly charged ion leads to the kinematical constraints for the $(e,2e)$ reaction (solid line in Fig. 2). This classical domain has been found also in a recent quasiclassical calculation by Goreslavski and Popruzhenko [11].

In Fig. 2 the parallel momentum correlation spectrum is presented for electron pairs emitted from an Ar atom during a 0.25 PW/cm$^2$ laser pulse. The large portion of events outside the $(e,2e)$-allowed regime now leads us to the excitation-tunneling model. Again, the observed electron momenta consist of the drift momentum and the initial momentum but, in contrast, now the electrons start at different times $t_1$ (recollision) and $t_2$ (tunneling) and, thus, gain different drift momenta. The first, recolliding electron excites its parent ion yielding an initial momentum $|\vec{p}_1(t_1)| = \sqrt{2E_{\mathrm{exc}}}$. The second, excited electron subsequently tunnels at a time $t_2$ and receives only drift momentum since the initial momentum for tunneling can be neglected.

Based on this scenario we can now derive the kinematical constraints for the correlated parallel electron momenta. For a given phase $\omega t_1$ the final momentum of the recolliding electron is restricted by $p_{\mathrm{drift}}(\omega t_1) - \sqrt{2E_{\mathrm{exc}}(t_1)} \le p^{\parallel}_{\mathrm{final}}(t_1) \le p_{\mathrm{drift}}(\omega t_1) + \sqrt{2E_{\mathrm{exc}}(t_1)}$, whereas the momentum of the second, tunneling electron is limited by $p^{\parallel}_{\mathrm{final}}(t_1) \le p^{\mathrm{max}}_{\mathrm{drift}} = 2\sqrt{U_P}$ with an expected maximum at $p^{\parallel}_{\mathrm{final}} = 0$. Here, $U_P = I/4\omega^2$ is the ponderomotive potential which corresponds to the mean quiver energy of an electron in the laser field with intensity $I$. The kinematically allowed region [shown in Fig. 1(b)] now has a rectangular shape and occurs fourfold due to the two half cycles of the laser field yielding opposite drift

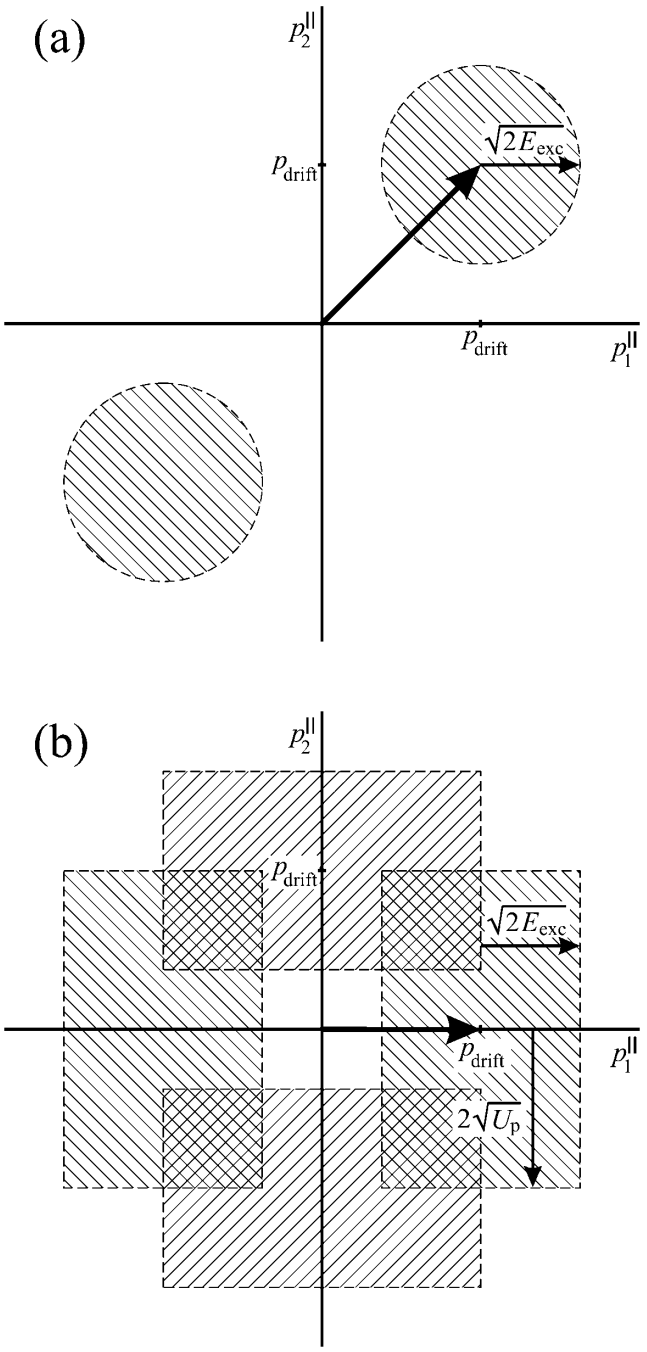


FIG. 1. Kinematically allowed regions (shaded areas) for the correlated electron momentum components $p_1^{\parallel}$, $p_2^{\parallel}$ parallel to the laser polarization axis. (a) Recollision $(e, 2e)$ process. (b) Recollision excitation with subsequent tunneling. See text for details.

momenta and due to the indistinguishability of the electrons. Superposition of these areas for all phases where the recollision energy exceeds the necessary excitation energy gives the total kinematically allowed region for the excitation-tunneling mechanism. Figure 2 illustrates that these kinematical constraints (dashed line) are in excellent accord with the experimental data. Of special interest is the symmetry of the correlation patterns for the two double

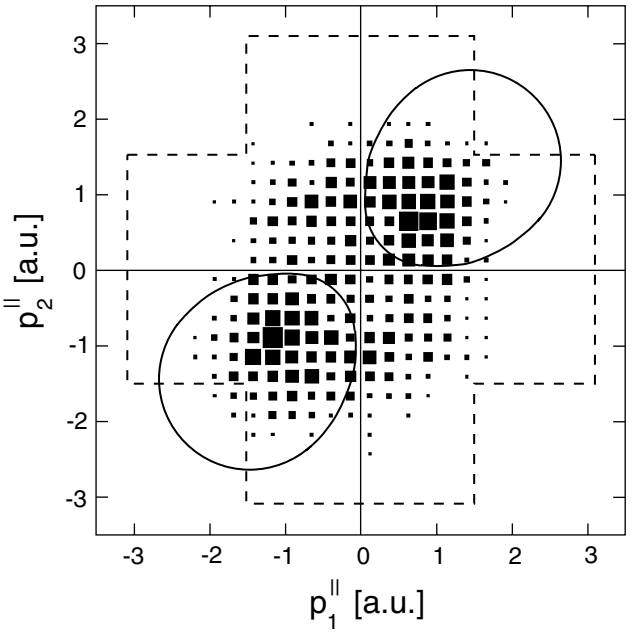


FIG. 2. Correlated electron momentum spectrum of two electrons emitted from Ar atoms at 0.25 PW/cm$^2$ for the parallel components $p_1^{\parallel}$, $p_2^{\parallel}$. The superposition of the kinematical constraints for all phases is shown for the recollision $(e, 2e)$ process (solid line) and for recollision excitation with subsequent tunneling (dashed line), respectively.

ionization mechanisms. Because of the fact that the electrons cannot be distinguished and the laser field defines only an alignment but not an orientation the correlation pattern for $p_1^{\parallel}$, $p_2^{\parallel}$ is symmetric with respect to both diagonals. In the case of the excitation-tunneling mechanism an additional symmetry with respect to the coordinate axes occurs because of the subsequent, independent emission of the electrons. For the $(e, 2e)$ mechanism this symmetry is broken due to the fact that both electrons acquire the same drift momentum.

Now, we discuss the filling of the "valley" in the ion momentum distribution parallel to the laser polarization direction. In the $p_1^{\parallel}$, $p_2^{\parallel}$ correlation spectrum the events due to the $(e, 2e)$ process are found only in the first and third quadrants. Based on the symmetry discussed above it is possible to obtain the full correlation pattern for the excitation-tunneling mechanism from the data in the second and fourth quadrants. This allows us to separate both mechanisms by subtracting the corresponding number of excitation-tunneling events from the measured number of all events in the first and third quadrants. Projection of the correlation pattern on the main diagonal gives the distribution for the parallel sum momentum $p_+^{\parallel} = p_1^{\parallel} + p_2^{\parallel}$, which reflects the parallel momentum spectrum of the doubly charged ions. Figure 3 shows these spectra separately for the different mechanisms. The $(e, 2e)$ process alone now leads to two clearly separated maxima close to the ion drift momentum of $4\sqrt{U_P}$, which is indicated

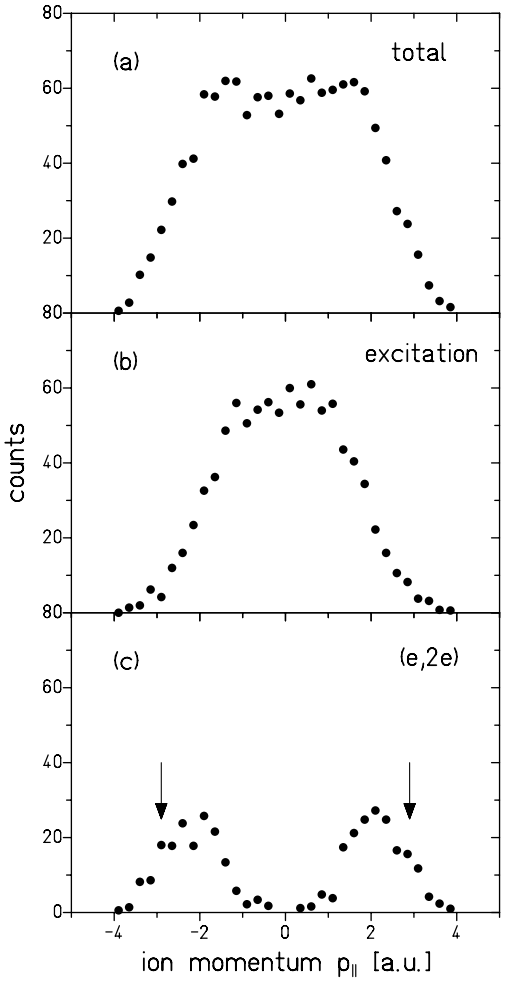


FIG. 3. Separation of the contributions of recollision ionization and excitation to the ion momentum distributions parallel to the laser polarization axis. Total ion momentum spectrum (a), recollision excitation with subsequent tunneling (b), and recollision $(e, 2e)$ process (c). The drift momentum $4\sqrt{U_P}$ for doubly charged ions is indicated by the arrows.

by the arrows. This is in good accord with our previous predictions based on simple classical considerations [9], as well as with recent quasiclassical calculations [11,13]. The second (excitation-tunneling) mechanism gives a single peak around zero momentum which dominates the total ion yield. Thus, the valley between the $(e, 2e)$ peaks is filled leading to the observed broad structure in the ion momentum distribution.

Finally, one may ask why the excitation mechanism in Ar at 0.25 PW/cm$^2$ is much more pronounced compared to Ne at 1.0 PW/cm$^2$ [5]. The reason may be twofold. First, the intensity normalized to the ionization potential is lower for $Ar^+$ ($I_P = 1.01$ a.u.) than for $Ne^+$ ($I_P = 1.51$ a.u.). Thus, the phase range where the recollision energy exceeds $I_P$ is reduced for Ar. Moreover, excitation and ionization by electron impact differ in their behavior at low impact energies. Whereas the ionization cross section approaches zero at threshold excitation may become increasingly probable. Second, $3p$-$3d$ excitations occur in Ar with large cross sections which are missing in Ne. The so-called "collapse" of the $3d$ orbital gives rise to large overlap with the $3p$ orbital yielding in very strong $3p$-$3d$ transitions which exceed the oscillator strength of $3p$-$4s$ transitions by a factor of 4 [18].

In conclusion, using a kinematical analysis of two-electron momentum correlation patterns for nonsequential double ionization of Ar in 0.25 PW/cm$^2$ laser pulses we are able to separate two different double ionization mechanisms. Both are based on the recollision of the first ionized electron with its parent ion core. In addition to the $(e, 2e)$ mechanism we identified excitation of the parent ion during the recollision with subsequent tunnel ionization of the excited electron as a second, dominant mechanism. This model explains the shape of observed ion momentum distributions and demonstrates the importance of excitation tunneling for nonsequential double ionization of Ar.

The experiments were supported by the Leibniz-Program of the Deutsche Forschungsgemeinschaft DFG. Support from GSI is gratefully acknowledged. We thank R. Dörner and W. Becker for fruitful discussions.

[1] A. L'Huiller, A. L'Lompre, G. Mainfray, and C. Manus, Phys. Rev. A **27**, 2503 (1983).
[2] L. F. DiMauro and P. Agostini, Adv. At. Mol. Opt. Phys. **35**, 79 (1995).
[3] J. Ullrich *et al.,* J. Phys. B **30**, 2917 (1997); R. Dörner *et al.,* Phys. Rep. **330**, 96 (2000).
[4] Th. Weber *et al.,* Phys. Rev. Lett. **84**, 443 (2000).
[5] R. Moshammer *et al.,* Phys. Rev. Lett. **84**, 447 (2000).
[6] Th. Weber *et al.,* J. Phys. B **33**, L127 (2000).
[7] D. N. Fittinghoff, P. R. Bolton, B. Chang, and K. C. Kulander, Phys. Rev. Lett. **69**, 2642 (1992).
[8] U. Eichmann *et al.,* Phys. Rev. Lett. **84**, 3550 (2000).
[9] B. Feuerstein, R. Moshammer, and J. Ullrich, J. Phys. B **33**, L823 (2000).
[10] P. B. Corkum, Phys. Rev. Lett. **71**, 1994 (1993).
[11] S. P. Goreslavski and S. V. Popruzhenko, Opt. Express **8**, 395 (2001).
[12] A. Becker and F. H. M. Faisal, Phys. Rev. Lett. **84**, 3564 (2000).
[13] R. Kopold, W. Becker, H. Rottke, and W. Sandner, Phys. Rev. Lett. **85**, 3781 (2000).
[14] M. Lein, E. K. U. Gross, and V. Engel, Phys. Rev. Lett. **85**, 4707 (2000).
[15] Th. Weber *et al.,* Nature (London) **405**, 658 (2000).
[16] H. van der Hart, J. Phys. B **33**, L699 (2000).
[17] R. Moshammer *et al.,* Nucl. Instrum. Methods Phys. Res., Sect. B **108**, 425 (1996).
[18] A. Hibbert and J. E. Hansen, J. Phys. B **27**, 3325 (1994).